Virologica Sinica 38 (2023) 922–930

Contents lists available at ScienceDirect

Virologica Sinica

journal homepage: www.keaipublishing.com/en/journals/virologica-sinica
www.virosin.org

Research Article

Ebola virus VP35 perturbs type I interferon signaling to facilitate viral replication

Zengguo Cao [a,1], Chenchen Liu [a,b,1], Cheng Peng [c,1], Yong Ran [c], Yulin Yao [a], Gengfu Xiao [a], Entao Li [d], Zixi Chen [e], Xia Chuai [a], Sandra Chiu [d,*]

[a] Key Laboratory of Special Pathogens and Biosafety, Wuhan Institute of Virology, Center for Biosafety Mega-Science, Chinese Academy of Sciences, Wuhan, 430071, China
[b] University of Chinese Academy of Sciences, Beijing, 100190, China
[c] National Biosafety Laboratory, Chinese Academy of Sciences, Wuhan, 430020, China
[d] Division of Life Sciences and Medicine, University of Science and Technology of China, Hefei, 230026, China
[e] Shenzhen Key Laboratory of Marine Bioresource and Eco-environmental Science, Shenzhen Engineering Laboratory for Marine Algal Biotechnology, Guangdong Provincial Key Laboratory for Plant Epigenetics, College of Life Sciences and Oceanography, Shenzhen University, Shenzhen 518060, China

ARTICLE INFO

Keywords:
Ebola virus (EBOV)
Type I interferon (IFN) signaling
Viral replication

ABSTRACT

As one of the deadliest viruses, Ebola virus (EBOV) causes lethal hemorrhagic fevers in humans and nonhuman primates. The suppression of innate immunity leads to robust systemic virus replication of EBOV, leading to enhanced transmission. However, the mechanism of EBOV-host interaction is not fully understood. Here, we identified multiple dysregulated genes in early stage of EBOV infection through transcriptomic analysis, which are highly clustered to Jak-STAT signaling. EBOV VP35 and VP30 were found to inhibit type I interferon (IFN) signaling. Moreover, exogenous expression of VP35 blocks the phosphorylation of endogenous STAT1, and suppresses nuclear translocation of STAT1. Using serial truncated mutations of VP35, N-terminal 1–220 amino acid residues of VP35 were identified to be essential for blocking on type I IFN signaling. Remarkably, VP35 of EBOV suppresses type I IFN signaling more efficiently than those of Bundibugyo virus (BDBV) and Marburg virus (MARV), resulting in stable replication to facilitate the pathogenesis. Altogether, this study enriches understanding on EBOV evasion of innate immune response, and provides insights into the interplay between filoviruses and host.

1. Introduction

Ebola virus (EBOV) is a highly virulent pathogen that belongs to the genus *Ebolavirus*, family *Filoviridae*, posing a significant public health concern. The 2013–2016 EBOV disease (EVD) epidemic resulted in over 28,000 cases and 11,000 deaths (Rasmussen, 2018; Wang et al., 2021) (https://www.cdc.gov/vhf/ebola/outbreaks/2014-west-africa/index.html). The *Ebolavirus* genus comprises six distinct species: Zaire ebolavirus (known as EBOV), Sudan virus (SUDV), Bundibugyo virus (BDBV), Tai Forest virus (TAFV), Bombali virus (BOMV), and Reston virus (RESTV) (Baseler et al., 2017). All the above-mentioned members of the *Ebolavirus* genus (except RESTV) can cause disease in human, as well as Marburg virus (MARV), a member of the *Marburgvirus* genus (Batra et al., 2018; Jacob et al., 2020). In particular, EBOV and MARV are often associated with highly lethal outbreaks (Jacob et al., 2020; Rougeron et al., 2015).

EBOV is an enveloped, single-stranded, negative-sensed RNA virus with a genome approximately 19 kb in length. The genome encodes several proteins including NP (nucleoprotein), VP35, VP40, GP (glycoprotein), VP30, VP24, and L (large protein) from 3′ to 5′ terminus (Jacob et al., 2020). Additionally, during the viral lifecycle, two soluble proteins (sGP and ssGP) are produced as a result of transcriptional editing frame shift of the *GP* gene (Mehedi et al., 2011; Sanchez et al., 1996). NP, VP35, VP30, and L interact with the viral genome, forming the viral ribonucleoprotein (RNP) complex (Feldmann et al., 2003). As a glycoprotein, GP is important for EBOV entry (Takada et al., 1997). VP40 is essential to mediate viral budding (Panchal et al., 2003), whereas VP24 facilitates nucleocapsid assembly (Hoenen et al., 2006; Huang et al., 2002).

As the first line of host defense, the innate immune response plays an indispensable role in the evolutionary arm race between virus and host. Type I interferon (IFN) response is a crucial aspect of the innate immune

* Corresponding author.
E-mail address: qiux@ustc.edu.cn (S. Chiu).
[1] Zengguo Cao, Chenchen Liu and Cheng Peng contributed equally to this work.

https://doi.org/10.1016/j.virs.2023.10.004
Received 13 June 2023; Accepted 8 October 2023
Available online 13 October 2023

response, which helps the host cells combat the virus during the initial stage of infection (Koyama et al., 2008). After the detection of pathogen-associated molecular patterns, multiple host pattern recognition receptors trigger the type I IFN production (Meylan et al., 2006). Then the secreted type I IFNs (including IFN-α and IFN-β) bind to the IFN receptor (IFNAR) in autocrine/paracrinely manners (Novick et al., 1994), and the signal activates type I IFN signaling pathway through Janus kinase (Jak)-signal transducer and activator of transcription protein (STAT) pathway, resulting in the expression of various IFN stimulated genes (ISGs) (Schoggins, 2014). However, virus has evolved various strategies to evade the host antiviral response, resulting in efficient viral replication (which usually leads to severe disease, and even death) (Shen et al., 2021). For filovirus, VP24 and VP35 are two main antagonists of host antiviral response (Ramanan et al., 2011). In addition, VP40 was also reported for its evasion ability of innate immune response (Ramanan et al., 2011; Valmas et al., 2010).

Although previous studies have identified several filoviral proteins that inhibit innate immune response through different signaling, comprehensive comparison studies of EBOV-encoding proteins are lacking. Here, we identified EBOV hijacks Jak-STAT signaling by transcriptomic analysis. By screening, we find VP35 and VP30 inhibit type I IFN signaling, and further analyses suggest that VP35 of EBOV suppresses type I IFN signaling more efficiently than another two filoviruses, resulting in stable replication to facilitate viral pathogenesis.

2. Materials and methods

2.1. Plasmids, cells and viruses

The pcDNA3.1-EBOV minigenome was constructed according to the strategy used previously (Tao et al., 2017). And the other EBOV minigenome (MG)-related plasmids (including pCAGGS-NP, pCAGGS-VP35, pCAGGS-VP30, pCAGGS-L) were gifted by Dr. Xinglou Yang from Wuhan Institute of Virology.

Huh-7, HEK293T, HeLa, and Vero E6 cell lines (ATCC® CRL-1586™) were purchased from the American Type Culture Collection, and maintained in high-glucose Dulbecco's modified Eagle's medium (DMEM) (Cat#C11965500BT, Gibco, USA) containing 10% fetal bovine serum (FBS) (Hyclone, USA) and 1% penicillin/streptomycin (Cat#15140122, Gibco) at 37 °C in a 5% CO_2 incubator.

The EBOV strain (Makona-C07, GenBank accession no. KJ660347.2) is stored at the Wuhan Institute of Virology, Chinese Academy of Sciences.

2.2. EBOV infection assays

All virus infections were performed in biosafety level 4 (BSL-4) laboratory of the National Biosafety Laboratory (Wuhan), Chinese Academy of Sciences. For RNA-seq, Huh-7 cells were infected with EBOV at a multiplicity of infection (MOI) of 1, followed by cellular RNA extraction and RNA-seq. To test if type I IFN treatment affected EBOV infection, Huh-7 and HeLa cells were infected with EBOV at different MOIs, and at 24 h post-infection (h.p.i.), the cells were treated with human IFN-α (1000 U/mL) for another 48 h. And then the supernatants were harvested for titration, and intracellular viral RNA levels were evaluated by RT-qPCR. In order to test mRNA levels of ISGs upon viral infection, Huh-7 cells were infected with EBOV at MOI of 1 and 0.1. At 24 h.p.i., the cells were treated or un-treated with human IFN-α (1000 U/mL) for 16 h, and cellular RNA was extracted for further evaluation.

2.3. Virus titration

EBOV titers were determined by $TCID_{50}$ assay on Vero E6 cells. Briefly, viral samples were prepared by 10-fold serial dilution in DMEM with 2% FBS, and 0.1 mL of each dilution was added into wells of 96-well-plates. After 1 h of viral adsorption at 37 °C, the inoculum was removed and fresh DMEM containing 2% FBS was added into each well. After two weeks, the viral titers were determined by cytopathy and expressed as the fifty percent of tissue culture infective dose per mL ($LgTCID_{50}$/mL), according to the method of Reed and Muench (L.J. Reed, 1938).

2.4. EBOV infection for RNA-seq

Huh-7 cells were seeded in 6-well-plates (6×10^5 cells/well), and left overnight at 37 °C to adhere. Huh-7 cells were either mock infected or infected with EBOV at an MOI of 1 for 1 h, and then the inoculum was removed and replaced with fresh DMEM containing 2% FBS. At 4 h.p.i. and 24 h.p.i., samples were harvested for cellular RNA extraction. RNA-seq was performed by Novogenne Co.Ltd (China). Briefly, mRNA was purified from total RNA, and was used for the generation of sequencing libraries. After clustering using TruSeq PE Cluster Kit v3-cBot-HS (Cat#PE-401-3001, Illumia, USA), the library preparations were sequenced on an Illumina Nova platform (Illumia, USA) and 150 bp paired-end reads were generated. Index of the reference genome was built using Hisat2 v2.0.5 and paired-end clean reads were aligned to the reference genome using software Hisat2 v2.0.5.

2.5. Type-I signaling luciferase reporter assay

Type-I signaling luciferase reporter assay was performed as described previously (Cao et al., 2021). Briefly, HEK293T or HeLa cells (1.5×10^5 cells per well in 24-well-plates) were co-transfected with 250 ng of ISRE promoter-driven *Firefly* luciferase reporter plasmid, 20 ng of *Renilla* luciferase control plasmid, and 100 ng of viral protein-expressing plasmid. At 16 h post-transfection (h.p.t.), cells were treated with human IFN-α (1000 U/mL) for 8 h. And then the cells were lysed and performed for dual-luciferase reporter assays according to the manufacturer's instructions of Dual Luciferase Reporter Assay Kit (Cat#DL101-01, Vazyme Biotech Co., Ltd, China).

2.6. Western blotting

Transfected or treated cells were harvested and lysed in IP lysis buffer (20 mmol/L Tris, 100 mmol/L NaCl, 0.05% n-Dodecyl β-D-maltoside, and protease inhibitor cocktail) with rotation at 4 °C for 1 h, then the lysates were clarified by centrifugation (12,000×*g* for 15 min at 4 °C). Clarified lysates were mixed with 4× lithium dodecyl sulfate buffer containing 100 mmol/L 1,4-dithiothreitol, and heated at 70 °C for 10 min. The proteins were resolved by SDS-polyacrylamide gel electrophoresis and transferred onto a PVDF membrane, followed by blocking, probing with indicated primary antibody and a secondary anti-rabbit/mouse IgG-peroxidase antibody (Supplementary Table S1). Chemiluminescent HRP Substrate (Cat# WBKLS0500, Merck Millipore, USA) was used for protein visualization.

2.7. Confocal microscopy

Vero E6 cells were seeded in sterile cover slips. At 24 h.p.t., the cells were treated with or without type I IFN (1000 U/mL) for 30 min, followed by three washes using phosphate-buffered saline (PBS). Then the cells were fixed with 4% paraformaldehyde and permeabilized with 1% Triton X100. After three times washes, the cells were blocking in PBS containing 2% FBS at room temperature for 1 h, then incubation with indicated primary antibodies (Supplementary Table S1) for 1 h, followed by three washes, and then staining with secondary antibodies (anti-mouse or anti-rabbit IgG conjugated with Alexa Fluor 488 or 568, Supplementary Table S1). Nuclei were stained with DAPI. Images were obtained by using a Zeiss LSM 800 Meta confocal microscope (Carl Zeiss, German).

2.8. Reverse transcription and quantitative RT-PCR (RT-qPCR)

Total intracellular RNA was prepared using QIAamp viral RNA mini-ikit (Qiagen, Valencia, CA, USA) according to the manufacturer's instructions. RNA was quantified using HiScript® II One Step qRT-PCR SYBR® Green Kit (Vazyme Biotech Co., Ltd, China). The primers used in this study were shown in Supplementary Table S2. The relative expression levels or fold changes of mRNA were calculated by $2^{-\Delta\Delta Ct}$ method using GAPDH mRNA as an internal control for normalization.

2.9. Minigenome assays

HEK293T cells (1×10^4 cells per well in 96-well-plates) were co-transfected with the following plasmids: pCAGGS-NP (31.25 ng), pCAGGS-VP35 (15.625 ng), pCAGGS-VP30 (9.375 ng), pCAGGS-L (125 ng), pcDNA3.1-EBOV minigenome with a *Firefly* luciferase reporter gene (62.5 ng), along with pCAGGS-T7 polymerase (31.25 ng) and control plasmid phRluc-TK encoding *Renilla* luciferase (2 ng). In some cases: pCAGGS-VP35 was replaced with tagged VP35-expressing plasmid, or plasmids encoding other filoviral VP35. At indicated time points post-transfection, cells were lysed and assayed for the luciferase activities according to the manufacturer's instructions of Dual Luciferase Reporter Assay Kit (Cat#DL101-01, Vazyme Biotech Co., Ltd, China).

2.10. Statistical analysis

Data were analyzed using GraphPad 8 software, and expressed as the mean ± standard deviation (SD). Statistical significance was calculated by Student's two-sided *t*-test, $*P < 0.05$, $**P < 0.01$, $***P < 0.001$, $****P < 0.0001$.

3. Results

3.1. EBOV infection is associated with dysregulation of ISGs

To better understand how EBOV usurps the host immune system to facilitate viral replication and pathogenesis, the transcriptome landscape of Huh-7 cells infected with EBOV was characterized. Using high-throughput RNA-seq, we identified multiple dysregulated genes between 4 h.p.i. and 24 h.p.i. (Fig. 1A, Supplementary Fig. S1, S2), and many genes with transcriptomic changes are highly clustered to Jak-STAT signaling, which is critical for EBOV infection (Fig. 1B).

IFN response partially constitutes Jak-STAT signaling (Stark and Darnell, 2012). In order to confirm whether IFN response plays an important role in suppression of EBOV infection, we used EBOV to infect Huh-7 and HeLa cells (MOI = 0.1 and 1), and then treated infected cells with human IFN-α. After another 24 h, CPE was observed (Supplementary Fig. S3). In addition, with IFN-α treatment, both viral titer and intracellular viral RNA were lower than those of mock–IFN–α treated group in two cell lines (Fig. 1C–F). These data suggest that type I IFN restricts EBOV infection. Since the antiviral function of type I IFN is due to effects of thousands of ISGs, which are derived from the activation of type I IFN signaling pathway, to study whether EBOV could block type I IFN signaling, we tested mRNA levels of several ISGs upon viral infection in Huh-7 cells. The results (Fig. 1G–J) suggest that EBOV efficiently inhibits the expression level of ISGs (including ISG15, ISG56, OAS1, and IFITM1) in a dose-dependent manner. Collectively, these data indicate that EBOV interacts with cellular processes, and the interaction perturbs the host immune system (such as type I IFN signaling) to facilitate viral pathogenesis.

3.2. EBOV proteins inhibit type I IFN signaling

We next sought to determine which viral proteins of EBOV antagonize type I IFN signaling. The expressing plasmids of viral proteins were used to screen their effects on type I IFN signaling using an ISRE-promoter-driven luciferase assay. As shown in Fig. 2A, five viral proteins significantly suppressed activation of ISRE promoter including VP35, VP40, VP30, VP24, and L. Due to the phosphorylation of STAT1 and STAT2 is necessary for type I IFN signaling, we examined viral suppression of STAT1/2 phosphorylation. We analyzed VP35, VP40, VP30, and VP24 because the suppression effects of these proteins on ISRE promoter activation are >45% (Fig. 2A). Data suggest that VP35, VP40, VP30, VP24 suppressed STAT1 phosphorylation by 31%–59%, whereas VP30 and VP24 inhibited STAT2 phosphorylation by 27% and 35%, respectively (Fig. 2B). Since phosphorylated STAT1/2 interact with IRF9 to form ISGF3 complex, which translocates to the nucleus to activate ISG transcription, we next tested the effect of viral proteins on STAT1 nuclear translocation. Consistent with their suppression on STAT1/2 phosphorylation, VP35, VP40, VP30, VP24 block STAT1 nuclear translocation of type I IFN signaling (Fig. 2C).

It has been documented how filoviral VP40 and VP24 function as IFN-antagonists (Mateo et al., 2010; Valmas et al., 2010), we verified that VP24 not only interacts with karyopherins, but also inhibits phosphorylation of STAT1/2 to block type I IFN signaling (Fig. 2A–C). Data from Fig. 2D and Supplementary Fig. S4 indicate that VP35 inhibits ISRE promoter activation dose-dependently in different cell lines, which prompted us to carry out subsequent research. Moreover, VP30 is also a newly identified viral protein which blocks type I IFN signaling (Fig. 2E and Supplementary Fig. S4).

3.3. VP35 transcripts increase rapidly at early stage of EBOV infection

Employing the RNA-seq dataset, a temporal atlas of the transcriptome in early stage of EBOV infection was constructed. These data were obtained by reference mapping reads against EBOV genome, followed by calculating and evaluating the read depth at each position. At 4 h.p.i., viral genes began to be expressed, while viral mRNA reached a relatively high level at 24 h.p.i. (Fig. 3A and Supplementary Fig. S5). Compared with other viral proteins, the transcript abundance of VP35 increased more rapidly from 4 h.p.i. to 24 h.p.i. (Fig. 3B), and the expression level of VP35 was relatively high (only was less than expression level of NP) among RNP complex-related proteins with type I IFN antagonistic activity (Fig. 3C). Altogether, the transcriptome results suggest that VP35 plays a vital role at early stage of EBOV infection.

3.4. VP35 suppresses type I IFN signaling via 1–220 amino acid residues

To investigate the key region of VP35 for type I IFN signaling antagonism, a series of truncated mutants were constructed (Fig. 4). Then, we evaluated the inhibitory function of the mutants using the type I IFN signaling luciferase reporter assay. The mutant with only the N-terminal 1–220 amino acid residues retains the inhibitory activity, but less than that of full-length VP35 (VP35-FL), while deletion of the N-terminal 1–220 amino acid residues can cause the mutant to fully lose inhibitory function (Fig. 4). However, the mutant deleted C-terminal 47 amino acid residues antagonizes type I IFN signaling in the same level of VP35-FL (Fig. 4). Collectively, the results indicate that N-terminal 1–220 amino acid residues of EBOV VP35 constitute the key domain for inhibitory ability of type I IFN signaling.

To identify the mechanism of VP35-induced type I IFN signaling suppression, we examined whether VP35 interacts with distinct components of type I IFN signaling (Supplementary Fig. S6). Data show that there is no component that interacts with VP35, indicating that VP35 inhibits type I IFN signaling pathway indirectly.

3.5. Inhibition of type I IFN signaling affects filovirus replication

We further compared the inhibiting ability of VP35 among EBOV, BDBV, and MARV. The result of Fig. 5A indicates that (1) the antagonism of VP35 on type I IFN signaling may be a pan-filoviral trait, because all

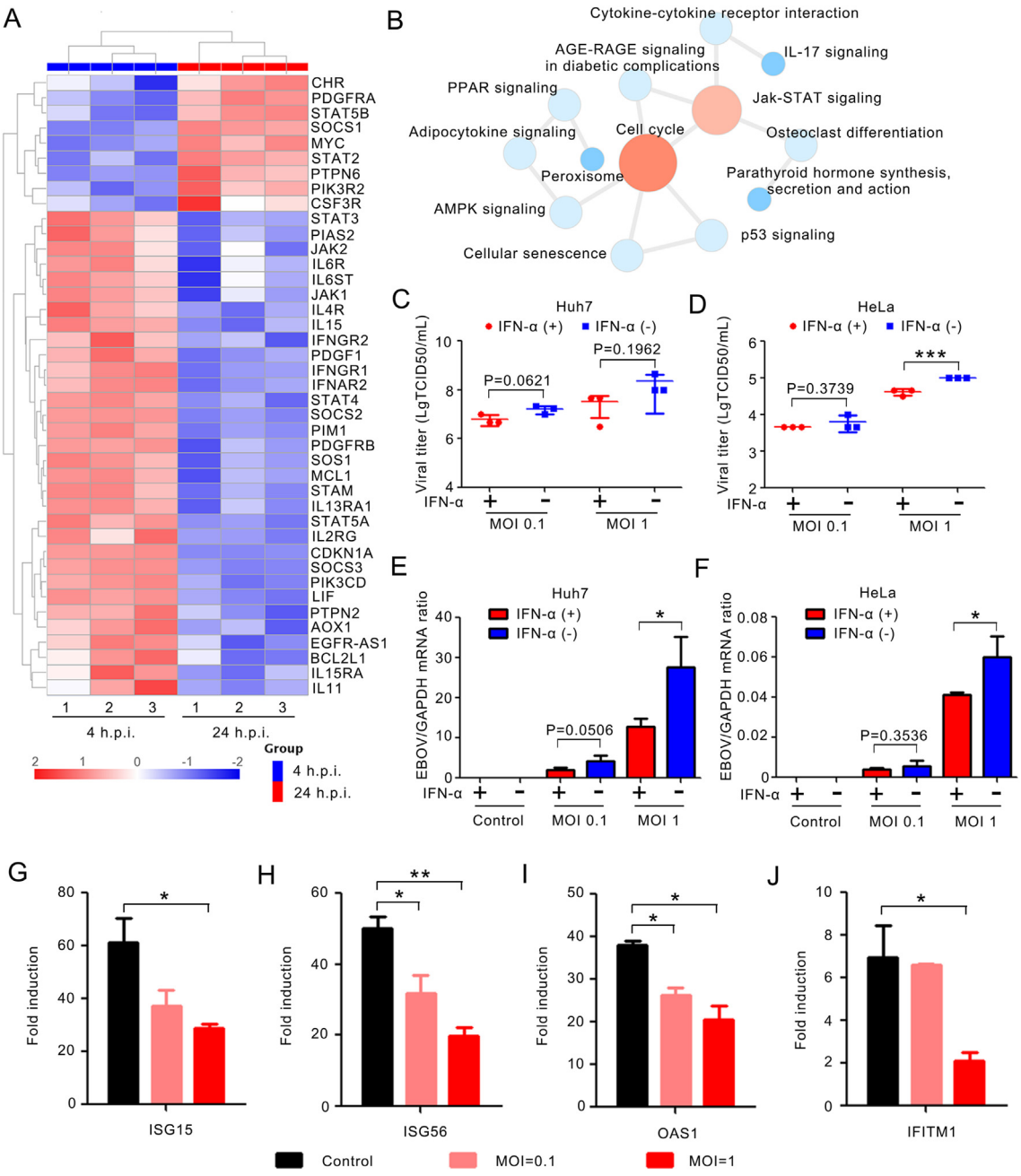

Fig. 1. EBOV infection is associated with dysregulation of ISGs. **A** Huh-7 cell were infected with EBOV at an MOI of 1 for 1 h, and then the inoculum was removed and replaced with fresh DMEM containing 2% FBS. At 4 h post infection (h.p.i.) and 24 h.p.i., samples were harvested for cellular RNA extraction. The heatmap was generated to visualize the fold change in expression levels of the target genes at 4 and 24 h.p.i. relative to mock infection group at the same time point, with up-regulated genes represented in red and down-regulated genes in navy. **B** Grouping of significant KEGG pathways based on up- or down-regulated gene. Each KEGG pathway is represented by a node, with the size of the node reflecting p-value of the pathway. **C–F** Huh-7 and HeLa cells were infected with EBOV at MOI of 0.1 and 1 respectively, uninfected cells were set as control, and the cells were treated with human IFN-α (1000 U/mL) at 24 h.p.i. After 48 h of IFN-α treatment, the supernatants were collected for titration, and the cells were harvested for total RNA extraction. Viral titers of Huh-7 cells (**C**) and HeLa cells (**D**) under indicated MOI were determined. And intracellular viral RNA levels in Huh-7 cells (**E**) and HeLa cells (**F**) were measured by RT-qPCR. The data were normalized to cellular GAPDH mRNA. **G–J** Huh-7 cells were mock-infected or infected with EBOV at indicated MOI. At 24 h.p.i., the cells were treated with human IFN-α (1000 U/mL), and cells without IFN-α treatment were also used. After another 16 h, total RNA extracted from cells was evaluated by RT-qPCR for the indicated genes. The data were analyzed by normalizing RNA levels to cellular GAPDH mRNA, and then normalizing to non- IFN-α treated samples to obtain fold induction. The data are presented as mean ± standard deviation (S.D.) from three biological replicates. Statistical significance was evaluated using a two-sided Student's *t*-test, $^{*}P < 0.05$, $^{**}P < 0.01$, $^{***}P < 0.001$.

VP35 from three different filoviruses could inhibit this pathway; (2) compared with EBOV, VP35 of BDBV or MARV was significantly weaker in antagonizing type I IFN signaling. In agreement with above results, EBOV VP35 inhibited phosphorylation of STAT1 more efficiently than those of the other two filoviruses (Fig. 5B).

To examine the biological relevance of the differences of VP35 in inhibiting type I IFN signaling among three filoviruses, we first evaluated the efficiency of EBOV minigenome with heterogeneous or tagged VP35. The results indicate that three VP35 fused with Myc-tag at C-terminus could support replication of EBOV minigenome at a comparable level

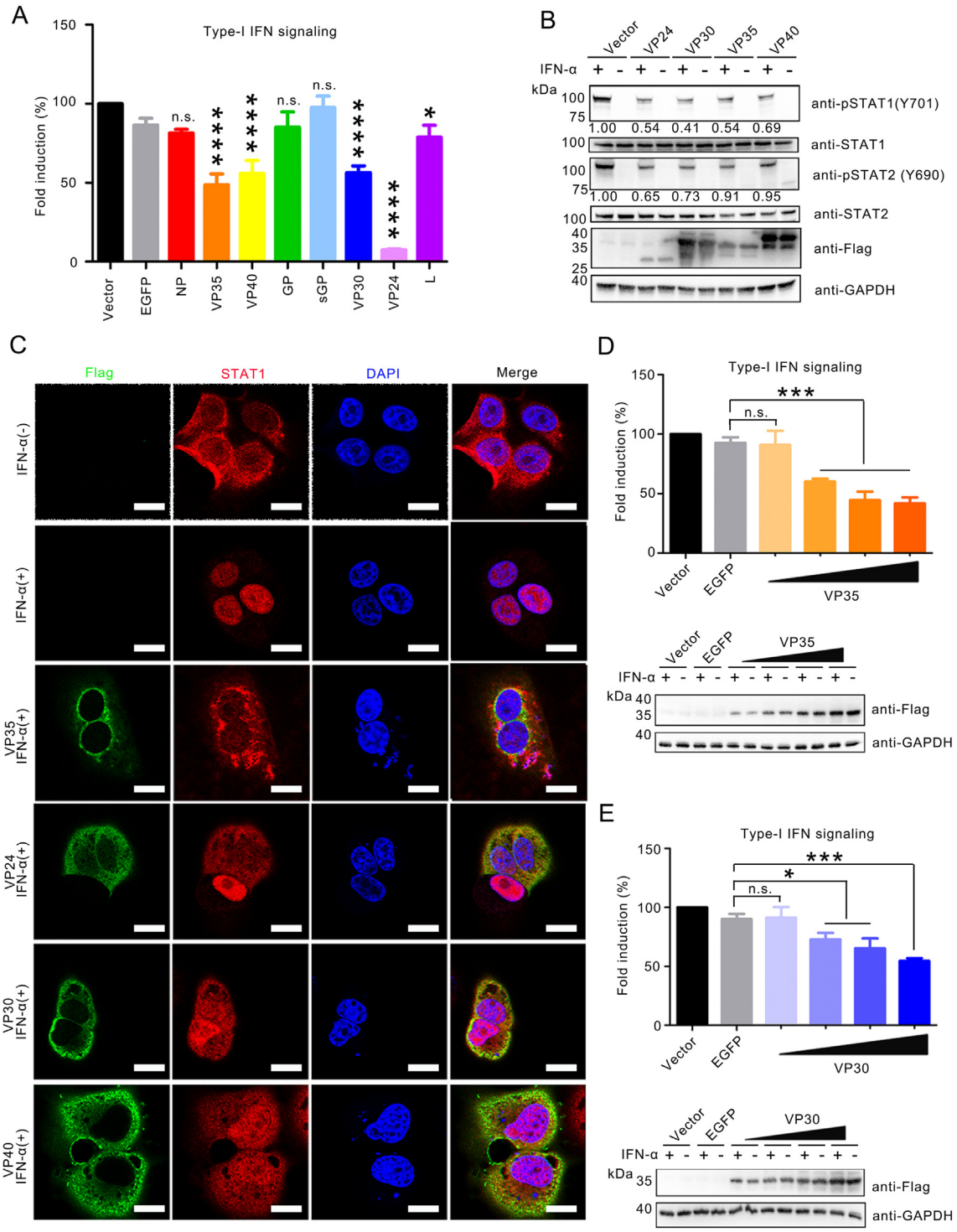

Fig. 2. EBOV proteins inhibit type I IFN signaling. **A** HEK293T cells were co-transfected with an ISRE promoter-driven *Firefly* luciferase reporter plasmid pISRE-luc, *Renilla* luciferase control plasmid phRluc-TK, and viral protein-expressing plasmids. At 16 h post transfection (h.p.t.), cells were treated with human IFN-α (1000 U/mL) for 8 h, followed by measurement of luciferase activity. The data were analyzed by normalizing *Firefly* luciferase values to *Renilla* luciferase values, and then normalized by non-stimulated samples to obtain fold induction. The value of empty vector control was set to 100%-fold induction. Error bars represent the mean ± S.D. **B** HEK293T cells were transfected with plasmids expressing the indicated viral protein, followed by human IFN-α treatment at a concentration of 1000 U/mL for 30 min. Then cells were harvested and analyzed by Western blotting. **C** Vero E6 cells were transfected with control plasmid or viral protein-expressing plasmid. Cells were treated with human IFN-α for 30 min at 24 h.p.t. And then, the cells were fixed and permeabilized for subsequent immunofluorescence analysis. Scale bar, 10 μm. **D** HEK293T cell were subjected to ISRE promoter luciferase assay described in (**A**). The inhibition efficiencies from different amounts of VP35 were shown in top, while protein expression levels using Western blotting are shown in bottom. **E** The methodology is the same as (**D**). The inhibition efficiencies from different amounts of VP35 were shown in top, while protein expression levels using Western blotting are shown in bottom. The data are presented as mean ± standard deviation (S.D.) from three biological replicates. Statistical significance was evaluated using a two-sided Student's *t*-test, $^{*}P < 0.05$, $^{***}P < 0.001$, n.s., no significance.

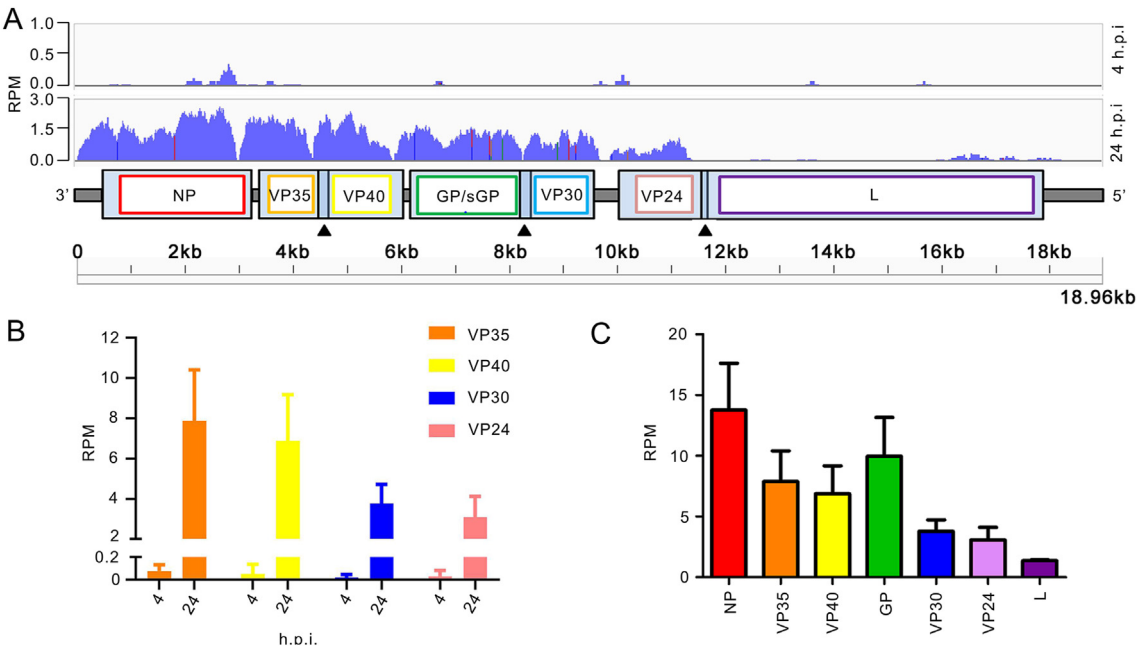

Fig. 3. VP35 transcripts increase rapidly at early stage of EBOV infection. **A** The transcription of EBOV in huh-7 cells was quantified at 4 h post infection (h.p.i.) and 24 h.p.i. by mapping RNA-seq reads against the EBOV genome sequence (shown at the bottom). The y-axis represents the number of reads per million mapped reads (RPM). **B** The expression levels of indicated viral proteins were analyzed in the transcriptome from 4 h.p.i. to 24 h.p.i, and the change in expression levels of these viral proteins over time are shown, with expression levels measured and displayed as reads per million (RPM) for each time point. **C** The expression levels of viral proteins were displayed as RPM, the data were analyzed in the transcriptome at 24 h.p.i. The data are presented as mean ± standard deviation (S.D.) from three biological replicates.

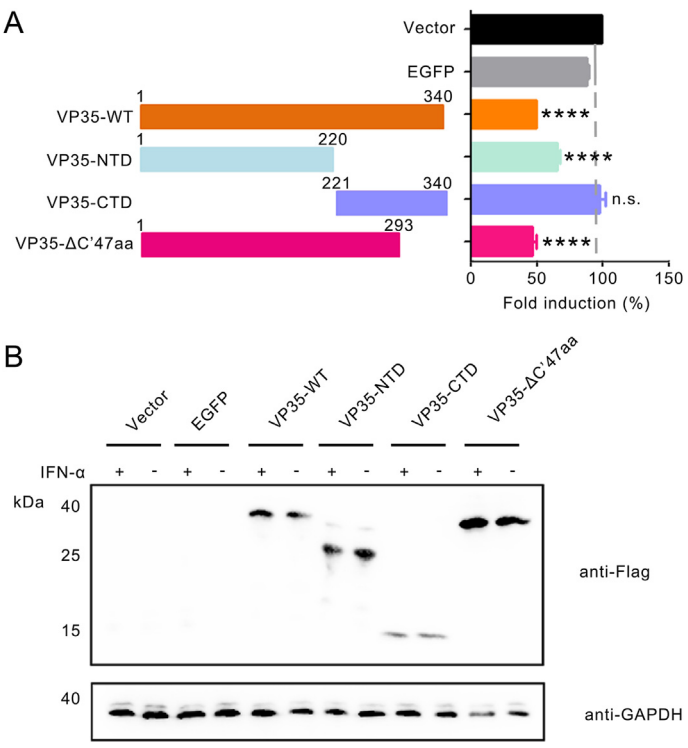

Fig. 4. VP35 suppresses type I IFN signaling via N-terminal 220 amino acid residues. **A** The plasmids expressing truncated mutants of EBOV VP35 were constructed, and used for ISRE promoter luciferase assay described in Fig. 2A. **B** Protein expression levels are analyzed by Western blotting. The data are presented as mean ± standard deviation (S.D.) from three biological replicates. Statistical significance was shown as ****P < 0.0001 or no significance (n.s.) through a two-sided Student's t-test.

(Fig. 5C). Next, we transfected three chimeric minigenomes into HEK293T cells, and then treated the cells with human IFN-α at 2 h.p.t., followed by analyzing luciferase activity of the cells at different time points after IFN-α treatment. We found that the minigenome with EBOV VP35-Myc produced higher replication efficiencies than the other two chimeric minigenomes at 2 h and 8 h after treatment with different concentrations of IFN-α (Fig. 5D and E), consistent with the finding that EBOV VP35 inhibited type I IFN signaling more efficiently than VP35 from BDBV and MARV. These above results demonstrated that VP35 antagonizes host type I IFN signaling to support filoviral replication at early stage of infection.

4. Discussion

Understanding viral inhibition mechanism of host innate immune response is critical to control epidemic of virus infection. Because of the BSL-4 restriction, the studies about EBOV infection need to be carried out restrictedly. The goals of this study are (1) to report a temporal atlas of the transcriptome at early phase of EBOV infection; (2) to identify and comprehensively compare EBOV-encoding proteins that antagonize type I IFN signaling; and (3) to compare the inhibition ability of viral proteins on type I IFN signaling among different filoviruses, and evaluate their functions on viral replication.

Upon infection, EBOV-induced multiple organ dysfunction syndrome is typical of EVD (Jacob et al., 2020; Martines et al., 2015), and liver injury is very common during EVD (Jacob et al., 2020), so we picked up a human liver cell line (Huh-7) for EBOV infection to characterize the transcriptome landscape. Among the dysregulated genes between 4 h.p.i. and 24 h.p.i., we enriched Jak-STAT pathway (Fig. 1A). This is not surprising because previous studies have documented several filoviral proteins that interfere host innate immune system, including Jak-STAT pathway (Jacob et al., 2020; Ramanan et al., 2011). Further studies are needed to make a connection of the suppressesed signaling pathways, and compare the viral proteins with inhibitory activities.

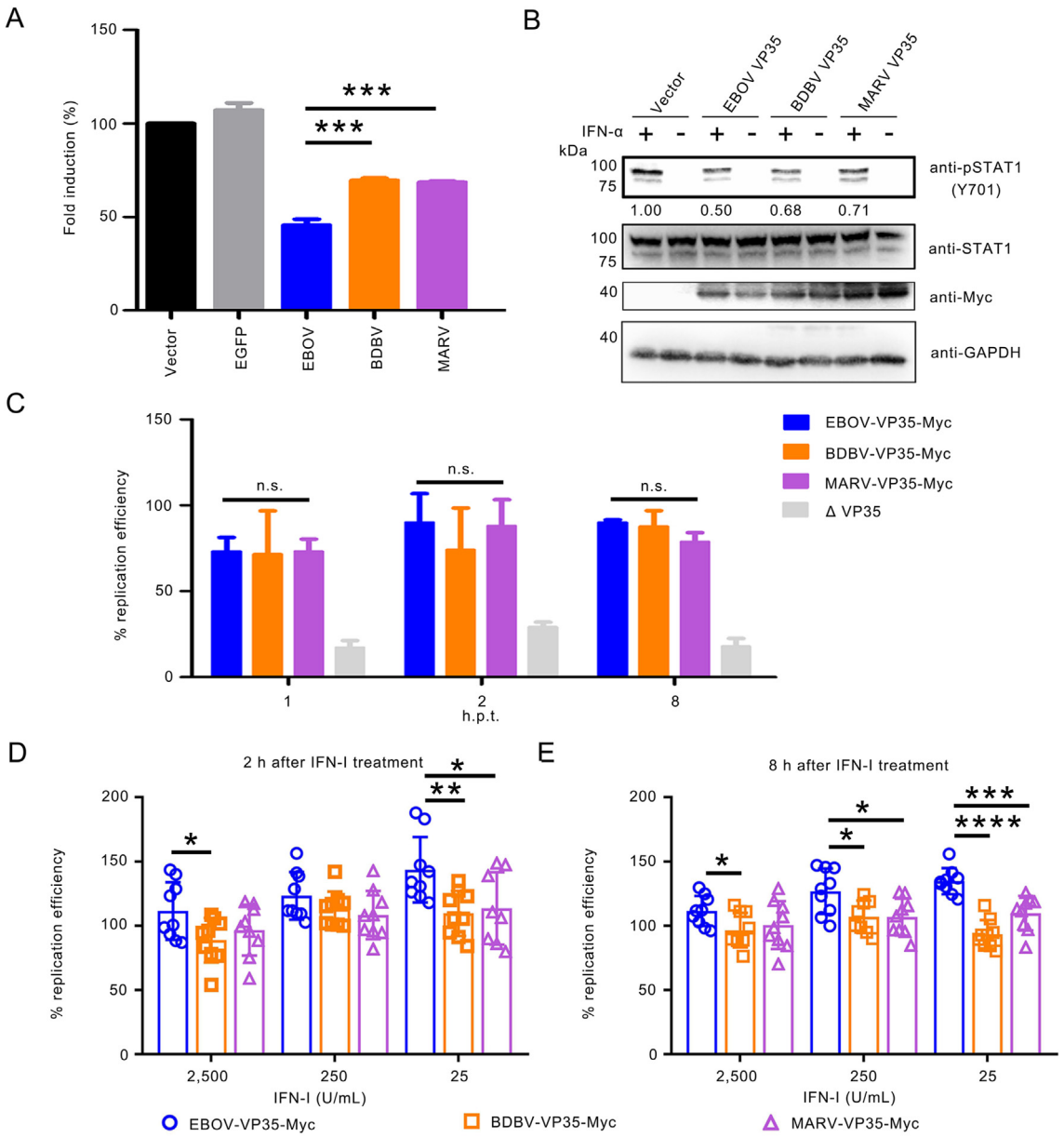

Fig. 5. Inhibition of type I IFN signaling affects filovirus replication. **A** Inhibitory efficacy of VP35 of EBOV, BDBV and MARV on type-I IFN signaling were compared. An ISRE promoter luciferase assay was performed in HEK293T cells, the details were described in Fig. 2A. **B** HEK293T cells were transfected with indicated viral protein-expressing plasmids, followed by treatment with 1000 U/mL human IFN-α at 24 h post transfection (h.p.t.) for 30 min. Cells were then harvested and analyzed by Western blotting. **C** VP35-WT of EBOV minigenome (MG) system (maternal MG) was replaced by EBOV-VP35-Myc, BDBV-VP35-Myc and MARV-VP35-Myc (chimeric MGs) respectively. EBOV MG system without VP35-expressing plasmid was used as control. At the indicated time points, luciferase activities were determined for evaluation of MG replication. Data was analyzed by normalizing *Firefly* luciferase to *Renilla* luciferase values, and then the ratio was relative to maternal MG ratio to obtain replication efficiency. **D, E** HEK293T cells were used for MG assays. Maternal and chimeric MGs were transfected into cells. The supernatants were replaced at 2 h.p.t. Human IFN-α with different concentrations were treated into each group. The replication efficiencies of 2 h (**D**) and 8 h (**E**) after IFN-α treatment were evaluated. The data are presented as mean ± standard deviation (S.D.) from three biological replicates. Statistical significance was evaluated using a two-sided Student's *t*-test, $^{*}P < 0.05$, $^{**}P < 0.01$, $^{***}P < 0.001$, $^{****}P < 0.0001$.

To comprehensively screen EBOV-encoding proteins for their inhibitory activities on type I IFN signaling, we used an ISRE-promoter-driven luciferase assay. We newly find VP35 and VP30 could antagonize type I IFN signaling significantly in two cell lines (Fig. 2D and E, Supplementary Fig. S4). After viral infection, the innate immune response is primarily triggered by the recognition of viral nucleic acid, then multiple components are activated in turn, and type I IFN genes are driven to transcription. Finally, the type I IFN is produced, and the above signal transduction process is named as type I IFN production. The secreted type I IFN is recognized by IFN receptor, and the downstream signal transduction is subsequently activated and signaled through Jak-STAT signaling. As a result, hundreds of ISGs are triggered to express, the type I IFN signaling is activated with antiviral function. Multiple groups determined EBOV VP35 inhibits type I IFN production pathway (Cardenas et al., 2006; Leung et al., 2009; Prins et al., 2009), but no study indicates VP35 functions in type I IFN signaling. Since the expression of antiviral ISGs results from the activation of type I IFN signaling pathway, we thought it is important to determine inhibitory mechanism of VP35 for uncovering immune evasion strategies of EBOV.

Consistent with a previous report (Wynne et al., 2017), polar sequential transcription was also observed at 24 h.p.i. (Fig. 3A, Supplementary Fig. S5). These data indicated VP35 transcript reached the

highest abundance among RNP complex-related proteins, suggesting that VP35 plays a vital role at early stage of EBOV infection. VP35 of EBOV could inhibit phosphorylation of STAT1 and STAT2 more efficiently than those of BDBV and MARV, and the biological relevance of this finding was evaluated through a reporter chimeric minigenome. Consistent with the greater inhibition of type I IFN signaling by EBOV VP35, the chimeric minigenome containing VP35 of BDBV or MARV was more sensitive to IFN-α inhibition.

In this study, we identified several viral proteins could antagonize multiple steps of type I IFN signaling, which explains the finding of a previous study that early postexposure treatment with type I IFN increased survival time of rhesus macaques infected with a lethal dose of EBOV (Smith et al., 2013). We have also provided evidence that with efficient transcription and translation, VP35 acts as an important type I IFN inhibitor to help EBOV hijack the host immune system for the establishment of stable replication at early stage during infection. Further study should focus on analyzing key amino acid sites for VP35 inhibitory function, which may serve as a potential target for anti-filovirus drug development.

5. Conclusions

In summary, we report a temporal atlas of the transcriptome in early stage of EBOV infection. We comprehensively screened viral proteins which antagonize multiple steps of type I IFN signaling, VP35 and VP30 are two newly identified EBOV-encoding proteins with inhibitory activities on type I IFN signaling. By using a reporter chimeric minigenome system, the biological relevance of VP35 activity was evaluated, the results suggest that the greater inhibition of type I IFN signaling by EBOV VP35, the chimeric minigenome containing VP35 of BDBV or MARV were more sensitive to IFN-α inhibition. Altogether, VP35 acts as an important type I IFN inhibitor to help EBOV hijack the host immune system for the establishment of stable replication at early stage during infection. Our findings add information to understanding of interaction between EBOV and the host, and suggest that VP35 may serve as a potential and promising target for future anti-filovirus drug development.

Data availability

All the data generated during the current study are included in the manuscript.

Ethics statement

This article does not contain any studies with human or animal subjects performed by any of the authors.

Author contributions

Zengguo Cao: conceptualization, investigation, methodology, software, data curation, formal analysis, visualization, writing-original draft, writing-review & editing, editing, funding acquisition. Chenchen Liu: data curation, formal analysis. Cheng Peng: investigation, methodology. Yong Ran: investigation, methodology. Yulin Yao: resources. Gengfu Xiao: project administration. Entao Li: investigation, data curation. Zixi Chen: methodology. Xia Chuai: investigation, data curation. Sandra Chiu: conceptualization, writing-review & editing, editing, project administration; resources, supervision, funding acquisition.

Conflict of interest

Prof. Sandra Chiu is an Editorial Board member for *Virologica Sinica* and was not involved in the editorial review or the decision to publish this article. The authors declare no competing interests.

Acknowledgements

We thank the BSL-4 Laboratory, Wuhan Institute of Virology, Chinese Academy of Sciences; the National Biosafety Laboratory (Wuhan), Chinese Academy of Sciences; the Center for Biosafety Mega-Science, Chinese Academy of Sciences; and the National Virus Resource Center for resource support. This work was jointly supported by the Strategic Priority Research Program of the Chinese Academy of Sciences (Grant No. XDB0490000) and the National Natural Science Foundation of China (82202521).

Appendix A. Supplementary data

Supplementary data to this article can be found online at https://doi.org/10.1016/j.virs.2023.10.004.

References

Baseler, L., Chertow, D.S., Johnson, K.M., Feldmann, H., Morens, D.M., 2017. The pathogenesis of ebola virus disease. Annual review of pathology 12, 387–418.
Batra, J., Hultquist, J.F., Liu, D., Shtanko, O., Von Dollen, J., Satkamp, L., Jang, G.M., Luthra, P., Schwarz, T.M., Small, G.I., Arnett, E., Anantpadma, M., Reyes, A., Leung, D.W., Kaake, R., Haas, P., Schmidt, C.B., Schlesinger, L.S., LaCount, D.J., Davey, R.A., Amarasinghe, G.K., Basler, C.F., Krogan, N.J., 2018. Protein interaction mapping identifies RBBP6 as a negative regulator of ebola virus replication. Cell 175, 1917–1930 e1913.
Cao, Z., Xia, H., Rajsbaum, R., Xia, X., Wang, H., Shi, P.Y., 2021. Ubiquitination of SARS-CoV-2 ORF7a promotes antagonism of interferon response. Cell. Mol. Immunol. 18, 746–748.
Cardenas, W.B., Loo, Y.M., Gale Jr., M., Hartman, A.L., Kimberlin, C.R., Martinez-Sobrido, L., Saphire, E.O., Basler, C.F., 2006. Ebola virus VP35 protein binds double-stranded RNA and inhibits alpha/beta interferon production induced by RIG-I signaling. J. Virol. 80, 5168–5178.
Feldmann, H., Jones, S., Klenk, H.D., Schnittler, H.J., 2003. Ebola virus: from discovery to vaccine. Nat. Rev. Immunol. 3, 677–685.
Hoenen, T., Groseth, A., Kolesnikova, L., Theriault, S., Ebihara, H., Hartlieb, B., Bamberg, S., Feldmann, H., Stroher, U., Becker, S., 2006. Infection of naive target cells with virus-like particles: implications for the function of ebola virus VP24. J. Virol. 80, 7260–7264.
Huang, Y., Xu, L., Sun, Y., Nabel, G.J., 2002. The assembly of Ebola virus nucleocapsid requires virion-associated proteins 35 and 24 and posttranslational modification of nucleoprotein. Mol. Cell 10, 307–316.
Jacob, S.T., Crozier, I., Fischer 2nd, W.A., Hewlett, A., Kraft, C.S., Vega, M.A., Soka, M.J., Wahl, V., Griffiths, A., Bollinger, L., Kuhn, J.H., 2020. Ebola virus disease. Nat. Rev. Dis. Prim. 6, 13.
Koyama, S., Ishii, K.J., Coban, C., Akira, S., 2008. Innate immune response to viral infection. Cytokine 43, 336–341.
Leung, D.W., Ginder, N.D., Fulton, D.B., Nix, J., Basler, C.F., Honzatko, R.B., Amarasinghe, G.K., 2009. Structure of the Ebola VP35 interferon inhibitory domain. Proc. Natl. Acad. Sci. U.S.A. 106, 411–416.
Martines, R.B., Ng, D.L., Greer, P.W., Rollin, P.E., Zaki, S.R., 2015. Tissue and cellular tropism, pathology and pathogenesis of Ebola and Marburg viruses. J. Pathol. 235, 153–174.
Mateo, M., Reid, S.P., Leung, L.W., Basler, C.F., Volchkov, V.E., 2010. Ebolavirus VP24 binding to karyopherins is required for inhibition of interferon signaling. J. Virol. 84, 1169–1175.
Mehedi, M., Falzarano, D., Seebach, J., Hu, X., Carpenter, M.S., Schnittler, H.J., Feldmann, H., 2011. A new Ebola virus nonstructural glycoprotein expressed through RNA editing. J. Virol. 85, 5406–5414.
Meylan, E., Tschopp, J., Karin, M., 2006. Intracellular pattern recognition receptors in the host response. Nature 442, 39–44.
Novick, D., Cohen, B., Rubinstein, M., 1994. The human interferon alpha/beta receptor: characterization and molecular cloning. Cell 77, 391–400.
Panchal, R.G., Ruthel, G., Kenny, T.A., Kallstrom, G.H., Lane, D., Badie, S.S., Li, L., Bavari, S., Aman, M.J., 2003. In vivo oligomerization and raft localization of Ebola virus protein VP40 during vesicular budding. Proc. Natl. Acad. Sci. U.S.A. 100, 15936–15941.
Prins, K.C., Cardenas, W.B., Basler, C.F., 2009. Ebola virus protein VP35 impairs the function of interferon regulatory factor-activating kinases IKKepsilon and TBK-1. J. Virol. 83, 3069–3077.
Ramanan, P., Shabman, R.S., Brown, C.S., Amarasinghe, G.K., Basler, C.F., Leung, D.W., 2011. Filoviral immune evasion mechanisms. Viruses 3, 1634–1649.
Rasmussen, A.L., 2018. Host factors involved in ebola virus replication. Curr. Top. Microbiol. Immunol. 419, 113–150.
Reed Hm, L.J., 1938. A simple method of estimating fifty per cent endpoints. Am. J. Hyg. 27, 493–497.
Rougeron, V., Feldmann, H., Grard, G., Becker, S., Leroy, E.M., 2015. Ebola and Marburg haemorrhagic fever. J. Clin. Virol. : the official publication of the Pan American Society for Clinical Virology 64, 111–119.
Sanchez, A., Trappier, S.G., Mahy, B.W., Peters, C.J., Nichol, S.T., 1996. The virion glycoproteins of Ebola viruses are encoded in two reading frames and are expressed through transcriptional editing. Proc. Natl. Acad. Sci. U.S.A. 93, 3602–3607.

Schoggins, J.W., 2014. Interferon-stimulated genes: roles in viral pathogenesis. Current opinion in virology 6, 40–46.
Shen, Q., Wang, Y.E., Palazzo, A.F., 2021. Crosstalk between nucleocytoplasmic trafficking and the innate immune response to viral infection. J. Biol. Chem. 297, 100856.
Smith, L.M., Hensley, L.E., Geisbert, T.W., Johnson, J., Stossel, A., Honko, A., Yen, J.Y., Geisbert, J., Paragas, J., Fritz, E., Olinger, G., Young, H.A., Rubins, K.H., Karp, C.L., 2013. Interferon-beta therapy prolongs survival in rhesus macaque models of Ebola and Marburg hemorrhagic fever. J. Infect. Dis. 208, 310–318.
Stark, G.R., Darnell Jr., J.E., 2012. The JAK-STAT pathway at twenty. Immunity 36, 503–514.
Takada, A., Robison, C., Goto, H., Sanchez, A., Murti, K.G., Whitt, M.A., Kawaoka, Y., 1997. A system for functional analysis of Ebola virus glycoprotein. Proc. Natl. Acad. Sci. U.S.A. 94, 14764–14769.
Tao, W., Gan, T., Guo, M., Xu, Y., Zhong, J., 2017. Novel stable ebola virus minigenome replicon reveals remarkable stability of the viral genome. J. Virol. 91, e01316-e01317.
Valmas, C., Grosch, M.N., Schumann, M., Olejnik, J., Martinez, O., Best, S.M., Krahling, V., Basler, C.F., Muhlberger, E., 2010. Marburg virus evades interferon responses by a mechanism distinct from ebola virus. PLoS Pathog. 6, e1000721.
Wang, R., Zhang, H., Peng, C., Shi, J., Zhang, H., Gong, R., 2021. Identification and characterization of a novel single domain antibody against ebola virus. Virol. Sin. 36, 1600–1610.
Wynne, J.W., Todd, S., Boyd, V., Tachedjian, M., Klein, R., Shiell, B., Dearnley, M., McAuley, A.J., Woon, A.P., Purcell, A.W., Marsh, G.A., Baker, M.L., 2017. Comparative transcriptomics highlights the role of the activator protein 1 transcription factor in the host response to ebolavirus. J. Virol. 91, e01174-17.